

# **Nanomagnet Arrays for Patterned Magnetic Media and Magnonic Crystal Applications**

**Manish Sharma**

**Final Report for Project AOARD-08-4023  
Asian Office of Aerospace Research and Development  
US Air Force**



**Centre for Applied Research in Electronics  
Indian Institute of Technology Delhi  
Hauz Khas, New Delhi - 110016.**

**31 August 2009**

## Report Documentation Page

*Form Approved*  
*OMB No. 0704-0188*

Public reporting burden for the collection of information is estimated to average 1 hour per response, including the time for reviewing instructions, searching existing data sources, gathering and maintaining the data needed, and completing and reviewing the collection of information. Send comments regarding this burden estimate or any other aspect of this collection of information, including suggestions for reducing this burden, to Washington Headquarters Services, Directorate for Information Operations and Reports, 1215 Jefferson Davis Highway, Suite 1204, Arlington VA 22202-4302. Respondents should be aware that notwithstanding any other provision of law, no person shall be subject to a penalty for failing to comply with a collection of information if it does not display a currently valid OMB control number.

1. REPORT DATE <b>27 NOV 2009</b>	2. REPORT TYPE <b>FInal</b>	3. DATES COVERED <b>04-06-2008 to 04-08-2009</b>	
4. TITLE AND SUBTITLE <b>Nanomagnet Arrays for Patterned Magnetic Media and Magnonic Crystal Applications</b>		5a. CONTRACT NUMBER <b>FA23860814023</b>	
		5b. GRANT NUMBER	
		5c. PROGRAM ELEMENT NUMBER	
6. AUTHOR(S) <b>Manish Sharma</b>		5d. PROJECT NUMBER	
		5e. TASK NUMBER	
		5f. WORK UNIT NUMBER	
7. PERFORMING ORGANIZATION NAME(S) AND ADDRESS(ES) <b>Indian Institute of Technology Delhi,Hauz Khas,New Delhi ,New Delhi ,IN, 110016</b>		8. PERFORMING ORGANIZATION REPORT NUMBER <b>N/A</b>	
9. SPONSORING/MONITORING AGENCY NAME(S) AND ADDRESS(ES) <b>AOARD, UNIT 45002, APO, AP, 96337-5002</b>		10. SPONSOR/MONITOR'S ACRONYM(S) <b>AOARD</b>	
		11. SPONSOR/MONITOR'S REPORT NUMBER(S) <b>AOARD-084023</b>	
12. DISTRIBUTION/AVAILABILITY STATEMENT <b>Approved for public release; distribution unlimited</b>			
13. SUPPLEMENTARY NOTES			
14. ABSTRACT <b>In this project, we have fabricated arrays of nanomagnets and characterized them for use as patterned media for high-density magnetic storage and as magnonic crystals in the microwave range. The nanomagnet arrays have been formed by electrodeposition in templates with feature sizes in the sub-100nm range using an electrodeposition system bought as part of this project. We have modelled the dynamic switching of the magnetizations in these arrays, and also done preliminary microwave absorption experiments on the nanowire arrays.</b>			
15. SUBJECT TERMS <b>magnetic storage, electrodeposition</b>			
16. SECURITY CLASSIFICATION OF:			17. LIMITATION OF ABSTRACT <b>Same as Report (SAR)</b>
a. REPORT <b>unclassified</b>	b. ABSTRACT <b>unclassified</b>	c. THIS PAGE <b>unclassified</b>	
			18. NUMBER OF PAGES <b>10</b>
			19a. NAME OF RESPONSIBLE PERSON

## SUMMARY SHEET

### 1. **Project Title: Nanomagnet arrays for patterned magnetic media and magnonic crystal applications**

### 2. **Project Objectives**

In this project, we have fabricated arrays of nanomagnets and characterized them for use as patterned media for high-density magnetic storage and as magnonic crystals in the microwave range. The nanomagnet arrays have been formed by electrodeposition in templates with feature sizes in the sub-100nm range using an electrodeposition system bought as part of this project. We have modelled the dynamic switching of the magnetizations in these arrays, and also done preliminary microwave absorption experiments on the nanowire arrays.

### 3. **Summary of Technical Work (details in Sec. 6):**

- a) Equipment:
  - a. Electrodeposition system purchased and installed.
  - b. Designed and custom-built a small, combined deposition and plasma oxidation chamber.
- b) Technical Progress:
  - a. Ferromagnetic Cobalt sheet films and nanowires grown using templated electrodeposition.
  - b. SQUID magnetometry measurements used to characterize nanowires. Results compared with micromagnetic modeling.
  - c. Preliminary microwave absorption experiments performed

### 4. **Conference Presentations:**

- a) S. Sharma, A. Barman, M. Sharma, L.R. Shelford, V.V. Kruglyak and R.J. Hicken, *Structural and magnetic properties of electrodeposited Co nanowire arrays*, IEEE Intermag Conference, Sacramento USA, May 2009.
- b) S. Singh, S. Pathak and M. Sharma, *Synthesis and Characterization of Magnetic Nanowires and Nanotubes*, International Workshop on Physics of Semiconductor Devices, Delhi India, Dec 2009.
- c) S. Pathak, S. Singh, R. Gaur and M. Sharma, *Synthesis of Cobalt Nanotubule Arrays and Characterization of Magnetization Dynamics*, International Conference on Nano Science and Technology, Mumbai India, Jan 2010.

### 5. **Journal Publications:**

- a) S. Sharma, A. Barman, M. Sharma, L.R. Shelford, V.V. Kruglyak and R.J. Hicken, *Structural and magnetic properties of electrodeposited Co nanowire arrays*, Solid State Comm. (to appear Oct. 2009).
- b) R. Gaur, S. Singh, S. Pathak and M. Sharma, Static and dynamic micromagnetic simulations of nanotubule arrays, IEEE Transactions on Magnetism (to appear in 2010).

## 6. Technical Work

### 6.1 Equipment

Two pieces of equipment were set up as part of this project: one, an electrodeposition system, and; two, a custom-built deposition-cum-oxidation chamber. These are described in the following discussion.

#### 6.1.1 Electrodeposition System

A Gamry potentiostat/ galvanostat based electrodeposition system was purchased and setup for performing the depositions. The system allows pulsed depositions at very low current levels, thus enabling us to control the deposition rate very precisely. This also allows one to do multi-element depositions from the same solution to form multilayered nanowires, which is part of continuing work that we shall be attempting in the future.

For using the system, we had to design a special electrochemical cell to mount the templates. The templates are very small in area around 1sqcm, and the small size of the nanopores means the actively conducting area during deposition is even smaller. For this reason, the concentration of the electrolyte solution had to be precisely controlled and the electrodes in the cell had to be placed close to each other. The design of the electrochemical cell is shown in the picture below.

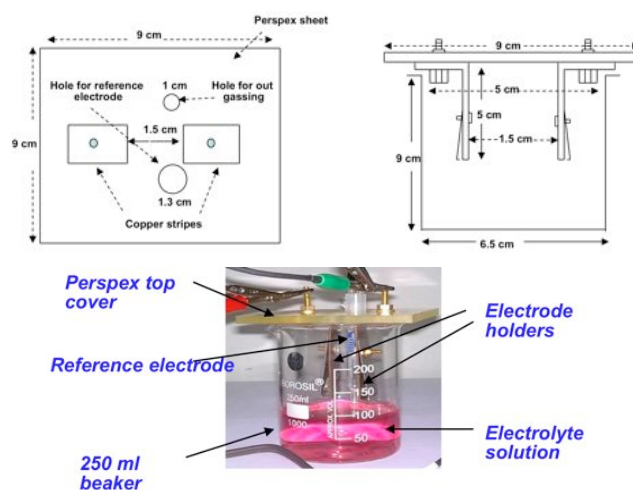


Figure: (top) Special electrochemical cell design. (bottom) Cell in operation.

The typical deposition process is depicted in the graphs in the Figure below. It is important to apply the right voltage to get the nanowire growth properly, and this is first determined using cyclic voltammetry performed on the working electrode with the electrolyte solution. After this, we usually grow a sheet film on a dummy sample, before proceeding to the final deposition in a template. The current is continuously monitored during deposition, and a sharp increase is typically seen once the nanopores fill up.

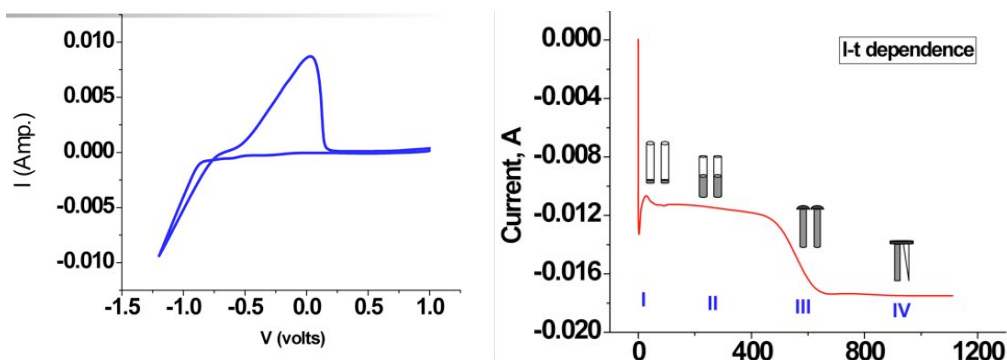


Figure: (left) Cyclic voltammogram of working electrode. (right) Current (A) vs. time (s) plot during templated deposition.

### 6.1.2 Deposition+Oxidation Chamber

To provide for controlled oxidation of the ferromagnetic films, a small vacuum chamber was built. This has a DC power supply and a cup-shaped electrode for producing DC glow discharge in an Ar+O<sub>2</sub> environment. The sample is attached to a floating substrate, to which a separate DC voltage bias can be applied, and placed upside down over the electrode. While the main working gas is Ar, a separate gas line is present for bleeding in small amounts of O<sub>2</sub>.



Figure: (left) Chamber with power supply. Substrate holder is to the left. (right) Chamber in operation with Cu deposition.

For the electrodeposition to be initiated, one needs to grow conductive seed layers on the back side of the template AAO/PCTE membrane. It is important for this film to be a metal of known electrochemical potential, and also for the film to be as smooth and thin as possible. A magnetron is used for DC sputtering of metal films. We have already used the chamber for Al, Au and Cu depositions. A Ni target is presently being fabricated as well.

### 6.2 Electrodeposited Nanowires and Nanotubules

We have been successful in forming nanowires with diameters down to 20nm and upto 20um in length. At the smaller diameters, the nanowires are solid and not hollow. The smallest hollow nanotubules that we have made are 50nm in diameter.

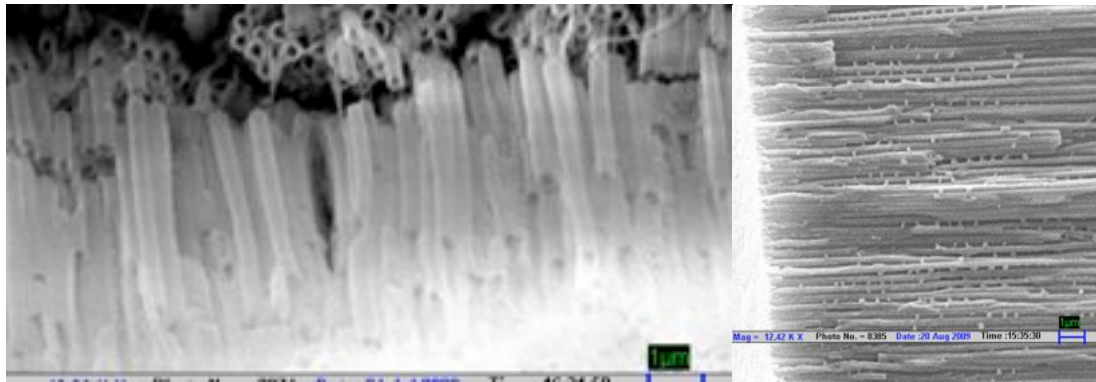


Figure: (left) Co nanotubes in template (right) cross-section SEM showing Co nanotubes inside template.

In order to verify that these nanotubes are indeed hollow, we took samples and dissolved the template. The released nanotubes were then collected and used for simple TEM imaging analysis. TEM images are shown in the Figure below. The transparency of the inner portions compared to the walls clearly indicates these are hollow. For smaller sized templates, one gets solid nanowires, which are also shown below.

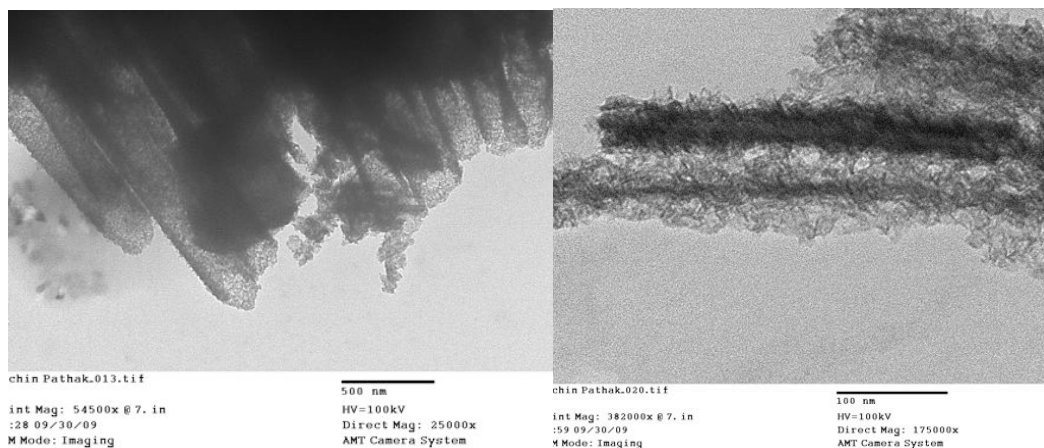


Figure: (left) TEM image of Hollow nanotubes of Co. (right) solid nanowires of Co.

There is a strong dependence on the deposition conditions (temperature, deposition voltage, concentration of solution and deposition rate) on whether hollow or solid nanostructures will form. At the moment, our effort is mainly to understand the influence of these conditions to achieve repeatable samples. This has previously been partially explained by other groups from a detailed electrochemical picture.

### 6.3 Measurements and Modelling

#### 6.3.1 SQUID measurements on nanowires and nanotubes.

The field dependent magnetization hysteresis was measured for cobalt nanowire array embedded in anodic alumina oxide membrane sample at room temperature by a Superconducting Quantum Interference Device (SQUID) magnetometer.

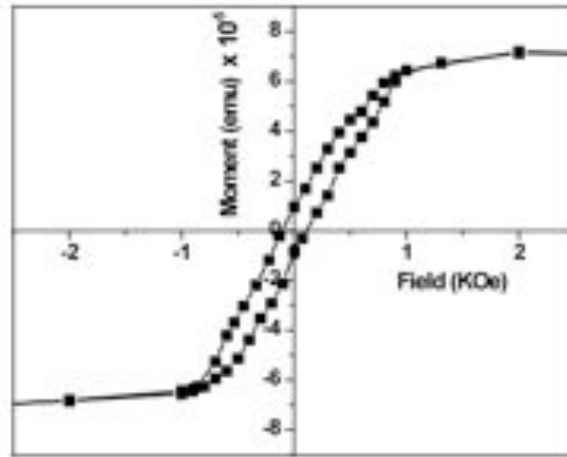


Figure: Hysteresis loop of cobalt solid nanowires embedded in AAO.

We found that the coercivity of cobalt nanowire array observed from this plot is 103 Oe. This is larger than coercivity value (10 Oe) for bulk cobalt material. This high coercivity value compared to the bulk material value indicates that the easy axis of magnetization is parallel to the nanowire axis and it arises because of high shape anisotropy due to the high aspect ratio of these nanostructures.

In order to check the loop arises only from nanowires in the template and not from extraneous deposition of magnetic material in the sample, we estimated the number of nanowires or pores in the template per unit area. Sample size was 2mm sq. with number of nanowires  $\sim 10^7$  (porosity of AAO used is  $10^9 \text{ cm}^{-2}$ ). We compared the number of nanowires deposited in our sample by calculating it from this hysteresis loop. Height of nanowire (T) calculated by equation  $T = \frac{M_w m}{AD}$  comes out to  $1.854 \mu\text{m}$ . Where A,  $M_w$ , m and D are the area of deposition, atomic weight, number of mole and density of metal deposited respectively. Volume of deposition observed from plot is  $4.92 \times 10^{-8} \text{ cm}^3$  (saturation magnetic moment / saturation magnetization of bulk cobalt). Number of nanowires calculated from this observation comes out to  $3.4 \times 10^6$  in a sample of area  $2 \text{ mm}^2$ . This value is smaller but still quite close to the number of nanowires expected ( $\sim 10^7$ ). This information rules out the chances of overdeposition of magnetic layer on nanowires. Thus, we can safely assume all of the magnetic signal in the SQUID loop comes directly from the nanowires.

### **6.3.2 Modelling work summary**

We used OOMMF and magpar finite-element modeling software for performing both static and dynamic micromagnetic simulations of nanowire and also nanotubule arrays. We first simulated for single nanowire and nanotubule, and then extended the simulations to arrays of nanowires and nanotubules to include realistic interaction effects in our models. The final goal of this modeling effort is to be able to calculate the dynamic response and fit FMR spectra as measured from high-frequency measurements.

### 6.3.2.1 Modelling of Static Response

Static micromagnetic calculations give us M-H curves that can be directly compared with experimental results from SQUID measurements. A typical SQUID measurement result is shown in Figure below. We note that the easy axis loop is tilted mainly due to an averaging of the coercivity effect over a large number of nanotubes.

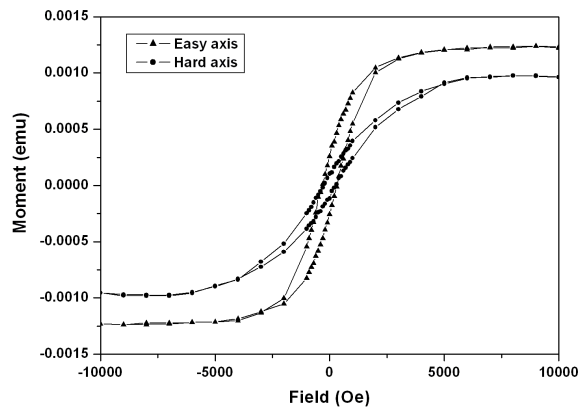


Figure: SQUID M-H loops along both the easy axis and hard axis. The above data are for 4µm long Co nanotubule arrays.

Results from the static magnetization calculations are shown in the two Figures below for a single nanotubule and for a nanotubule array. The easy axis coercivity of the nanotubule array is found to be slightly reduced than for a single nanotubule. This suggests that the interaction between neighbouring nanotubes is quite strong. The coercivity of the nanotubule array matches well with the experimentally observed coercivity in Figure above. There is a clear canting of the easy axis loop when averaged over seven nanotubes, and this matches the effect observed experimentally.

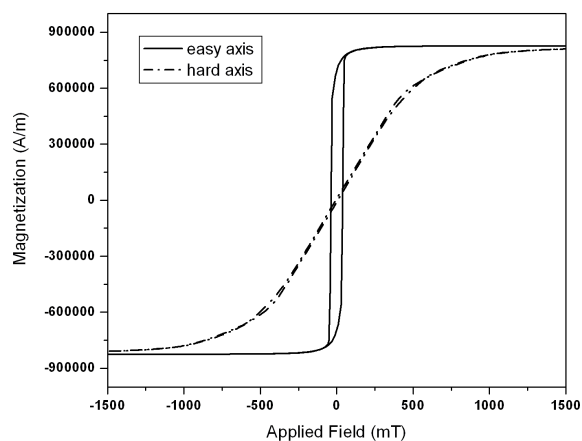


Figure: Magnetization loops along both the easy axis and hard axis for a single 3µm long Co nanotubule as calculated using micromagnetic simulations. The coercivity is 37.9 mT.

The hard axis loops in both Figure for a single 3µm long Co nanotubule and Figure (below) for an array of seven closely-packed 3µm long Co nanotubes, which show an anisotropy of around 500mT.

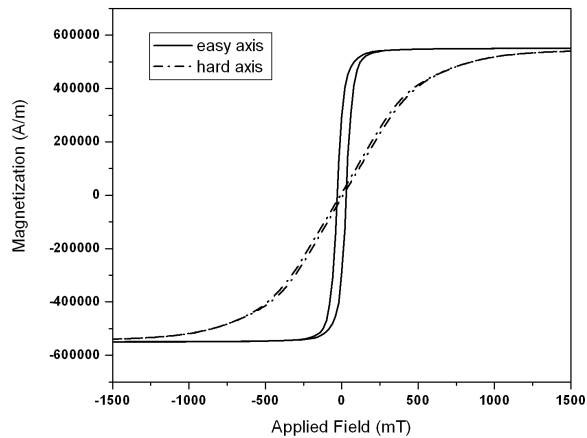


Figure: Magnetization loops along both the easy axis and hard axis for a close-packed array of  $3\mu\text{m}$  long Co nanotubes as calculated using micromagnetic simulations. The coercivity is reduced to 28.8 mT.

### 6.3.2.2 Modelling of Dynamic Response

Dynamic micromagnetic calculations were done by simulating a fast magnetic field pulse applied to the sample (first single nanotubule then a nanotubule array) in the transverse direction. The time-domain magnetization reversal curves were fourier-transformed to calculate the power spectrum as a function of frequency of excited FMR mode. As can be seen in Figure below, the dominant first FMR mode occurs at a reasonably high frequency of 22GHz. To compare, we also calculated the frequency for a solid nanowire array of the same dimensions and found it to be 14GHz. This suggests that the hollow centre affects greatly the propagation of the spin waves in the nanowire or the nanotubule.

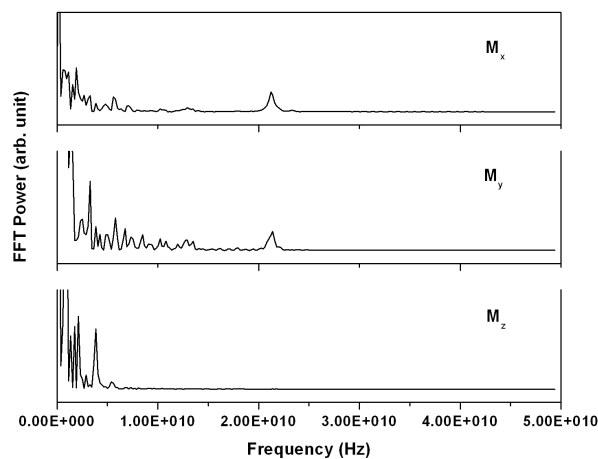


Figure: Calculated FMR modes of a  $3\mu\text{m}$  Co nanotubule array. The field is applied at 0 degrees. A dominant first FMR mode seen at 22GHz in the x- and y- axes.

Since both the direction and strength of the field can influence the generation of the spin wave along or across the nanotubule, we first varied the angle of the applied field from 0 to 85 degrees. The effect of this on each of the resonance modes is shown in Figure below. The effect of the strength of the magnetic field is to induce a faster

magnetic response in the sample, thus leading to the establishment of much stronger peaks. The shift of the modes is more or less linear towards higher frequencies. As an example of this trend, the first FMR mode (at 0 degree applied field angle) shifts from 22GHz for 0.2Tesla, to 30GHz for 0.4Tesla, and to around 34GHz for 0.6Tesla.

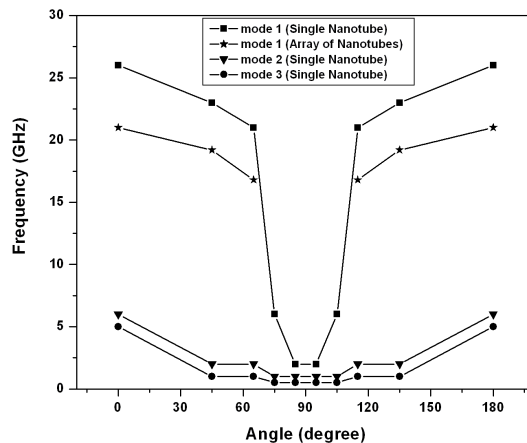


Figure: Effect of field angle on FMR modes for single nanotubule and nanotubule arrays

#### 6.4 Microwave absorption measurements

The synthesized nanowires can be used in two ways. One possible approach is by dissolving the template, collecting the nanowires and then redispersing them in a polymer or other matrix. This gives a reasonably random or only partially oriented packing of the nanowires but the density of nanowires can be varied depending on sample preparation. In a second approach, the electrodeposited template can be used directly. This is because it already has the nanowires arranged in a densely packed array, albeit the density is fixed depending on the template used.

Finally, when such templates will be used in making the inductor, one will have tuned absorption at specific frequencies. In particular, oriented nanowires arranged in arrays would have highly anisotropic response in different directions. This can also be studied by direct absorption of incident microwave energy on the nanowire array, if one were to mount the nanowire array sample inside a waveguide.

For these measurements, a single template (approx 0.5 x 0.5cm size) was inserted in a waveguide (of the appropriate band) as a sample. Absorption measurements were done using a vector network analyzer in the S (2-4GHz) , C(4-8GHz) , X(8-12GHz), and K (12-20GHz) bands. While some absorption was seen in the other bands as well, a prominent absorption in the C-band was seen around 4-5.6Ghz range. For more detailed measurements, we intend to use several templates and tile them together in the waveguide cross-section. It is also expected that there will be a strong angular dependence of the orientation of the nanowire arrays since they are all arranged parallel to each other in a close-packed array. Some indication of this is already present in our measurements. These results are not published yet.

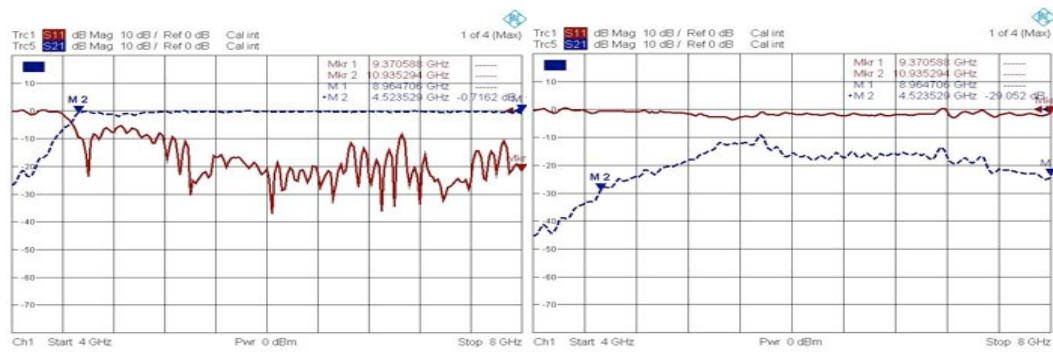


**Figure:** (left) Base response of C-band (4-8GHz) without sample. (right) Response with one template in place.

## 7. Conclusion

We have been able to grow solid nanowires and also hollow nanotubules of Co using electrodeposition. These nanostructures have been grown in close-packed arrays inside templates. Magnetic characterization performed on these films using SQUID magnetometry has been compared with micromagnetic modeling. The modeling also predicts the dynamic FMR response of the nanostructures at GHz frequencies. It has been found that there is absorption of microwaves in the C band, for which preliminary measurements have also been done. The structures